ICIC Express Letters
Volume **17**, Number **11**, November **2023**

ICIC International ©2023 ISSN 1881-803X
pp. **1225–1233**

CHANNEL REDUCED GENERALIZED LEGENDRE FILTER FOR NONLINEAR ACTIVE NOISE CONTROL

Xinnian Guo[1,2,*], Ziyang Kang[1,*], Guodong Zhu[1], Yang Shen[1], Lin Chen[1,2] and Hongyan Ding[1]

[1]School of Information Engineering
[2]Jiangsu Province Engineering Research Center of Smart Poultry Farming and Intelligent Equipment
Suqian University
No. 399, Huanghe South Road, Suqian 223800, P. R. China
{ 20200303123; 17109; 17045; 01013 }@squ.edu.cn
*Corresponding authors: { xinnianguo; 17127 }@squ.edu.cn

Received February 2023; accepted April 2023

Abstract. *In this paper, a channel reduced generalized Legendre (CRGL) filter and corresponding filtered-x least mean square (FXLMS) and filtered-error least mean square (FELMS) algorithms were proposed with applications in nonlinear active noise control (NANC). The filter was developed by adding the cross products to the orthogonal Legendre polynomials derived from the Volterra diagonal channel structure and updating the dominant channel weights. The computation complexity was analyzed and compared to validate the efficiency for the proposed CRGL filter and algorithms. Numerical simulation results demonstrate effectiveness of the proposed filter with the FXLMS and FELMS algorithms for nonlinear active noise control.*
Keywords: Active noise control, Adaptive filter, Adaptive algorithm, Generalized Legendre filter

1. **Introduction.** Vibration and noise was one of the main factors leading to fatigue damage to local structures of aircraft, submarines and industrial equipment. Therefore, noise control technology was widely used in military, industrial, automobile and other fields [1,2]. Passive control technology depending on the absorption or reflection characteristics of materials was first applied in various fields. However, it was difficult to meet the growing noise control demand for the reason that the passive noise control technology had the disadvantages of expensive materials, large volume and poor performance for low-frequency noise [1]. Active noise control (ANC) technology according to the superposition principle has inspired for its advantages of low cost, significant low-frequency performance and easy implementation. It is likely to become a standard technology for noise reduction in enclosed spaces in the future.

The linear solution of finite impulse response (FIR) filter equipped with the filtered-x least mean square (FXLMS) algorithm [3,4] has been widely applied in actual ANC systems. However, the real systems may contain nonlinear properties which come from the noise source, nonlinear primary and secondary paths. In the nonlinear cases, the linear solution suffered performance degradation or even failed. Therefore, nonlinear active noise control (NANC) technology was employed to process the nonlinearity [3-15]. The nonlinear adaptive filter was one of the most active research areas in NANC area. At present, the types of new filters mainly include function expansion filters [3-5], recursive filters [6,7] and bilinear filters [8,9]. The recursive and bilinear filters faced the challenges of heavy computational loads and unclear stability mechanism under the bounded input bounded output (BIBO) criterion.

DOI: 10.24507/icicel.17.11.1225

The function expansion filters were famous for the simple structure and super performance for handling nonlinearity from noise source and primary path. The Volterra [3] and functional link artificial neural network (FLANN) [4] filters were first proposed. To achieve better performance, several new filters have been developed, such as the generalized FLANN (GFLANN) filter [10], Legendre neural network (LeNN) filter [11], exponential functional link network (EFLN) filter [12], and generalized Chbyshev filter [13]. The Legendre filter expanding with Legendre expansions has been used in NANC with good results. However, it does not use cross-terms and thus its performance can be negatively affected when facing crossing nonlinearity in NANC. Therefore, one aim of our contribution is to modify the original Legendre structure to include cross-terms, which termed generalized Legendre filter. The heavy computational complexity caused by the cross-terms limits the applications. Therefore, we further proposed a channel reduced generalized Legendre (CRGL) filter implementation which applied the channel reduced strategy to reducing computational complexity [6-9,13,14]. The associated adaptive algorithm using FXLMS and filtered-error LMS (FELMS) structure was derived. Furthermore, the computational complexity compared with different filters and control performance under various nonlinear effects were conducted to show the comprehensive performance of the proposed filter and algorithms.

This paper is organized as follows. Section 2 proposes the CRGL filter. We derive the FXLMS and FELMS algorithms and compare the computational complexity in Section 3. Section 4 presents the computer simulations. Finally, the conclusion was given in Section 5.

2. **Channel Reduced Generalized Legendre Filter.** Legendre polynomials are a series of polynomials defined in the form of recursive equations. The recurrence relationship of adjacent three terms for original Legendre polynomials which is a system of complete and orthogonal polynomials is defined as follows:

$$l_n(x) = \frac{2n-1}{n} x l_{n-1}(x) - \frac{n-1}{n} l_{n-2}(x) \tag{1}$$

where $l_0(x) = 1$, $l_1(x) = x$, $l_2(x) = (3x^2 - 1)/2$.

However, many nonlinear systems exist cross characteristic. Therefore, a generalized Legendre filter with diagonal channel structure can be constructed based on Legendre polynomials. In order to ensure the algebraic integrity of the constructed polynomial structure, we multiply all the delay signals and remove the duplicates. The second order form of the generalized Legendre filter with diagonal channel was shown in Table 1.

Table 1. Channel input vectors of the generalized Legendre filter

Input vector	Elements
$\boldsymbol{L}_0(n)$	$x(n)$, $x(n-1)$, $x(n-2)$, $x(n-N+1)$
$\boldsymbol{L}_1(n)$	$\left[3x^2(n)-1\right]/2$, $\left[3x^2(n-1)-1\right]/2$, $\left[3x^2(n-2)-1\right]/2, \ldots, \left[3x^2(n-N+1)-1\right]/2$
$\boldsymbol{L}_2(n)$	$x(n)x(n-1), x(n-1)x(n-2), \ldots, x(n-N+2)x(n-N+1)$
$\boldsymbol{L}_3(n)$	$x(n)x(n-2), x(n-1)x(n-3), \ldots, x(n-N+3)x(n-N+1)$
$\ldots$	$\ldots$
$\boldsymbol{L}_N(n)$	$x(n)x(n-N+1)$

The output for the second order generalized Legendre filter is expressed as

$$y(n) = \boldsymbol{w}^T(n)\boldsymbol{l}(n) = \boldsymbol{W}_0^T(n)\boldsymbol{L}_0(n) + \boldsymbol{W}_1^T(n)\boldsymbol{L}_1(n) + \cdots + \boldsymbol{W}_N^T(n)\boldsymbol{L}_N(n) \tag{2}$$

where $\boldsymbol{w}(n) = [\boldsymbol{W}_0(n), \boldsymbol{W}_1(n), \ldots, \boldsymbol{W}_N(n)]$ designate the second order diagonal channel weight coefficients and $\boldsymbol{l}(n) = [\boldsymbol{L}_0(n), \boldsymbol{L}_1(n), \ldots, \boldsymbol{L}_N(n)]$ the input signals. As shown

in Figure 1, the signal vectors of $\boldsymbol{L}_2 \sim \boldsymbol{L}_N(n)$ which is time invariant are presented by diagonal channels for $N = 7$. The energy of the cross diagonal structure always centralized around the principles [14] in real systems, which lead to low calculation without sacrificing performance using the channel reduced structure. We implemented the cross sections by keeping the elements of a few main channels [13]. Assuming that M diagonal channels of (solid line channels in Figure 1) are remained for the generalized Legendre filter, the output of $y(n)$ can be renovated as

$$y(n) = \boldsymbol{w}^T(n)\boldsymbol{l}(n) = \boldsymbol{W}_0^T(n)\boldsymbol{L}_0(n) + \boldsymbol{W}_1^T(n)\boldsymbol{L}_1(n) + \cdots + \boldsymbol{W}_{M+1}^T(n)\boldsymbol{L}_{M+1}(n) \tag{3}$$

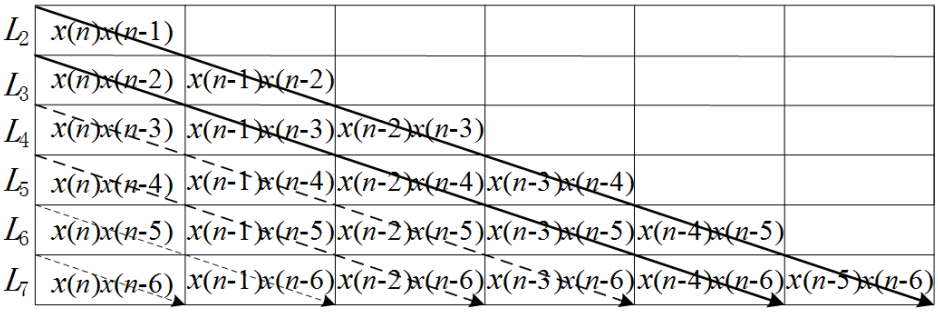

FIGURE 1. Diagonal channel of cross terms

3. Adaptive Algorithm.

3.1. Filtered-x LMS algorithm. The adaptive FXLMS algorithm based on the channel reduced generalized Legendre filter for NANC system is shown in Figure 2. $x(n)$ is the noise source collected by the primary microphone. $p(n)$ presented the primary transfer function, $d_p(n)$ is the acoustic noise transmitted through the primary path, $y(n)$ is the control signal generated by the processer, and $d_s(n)$ the secondary control signal transmitted through the secondary path noted as $\boldsymbol{s}(n)$. The error signal of $e(n)$ sensed by the error microphone was residual signal after superposition of the primary noise of $d_p(n)$ and secondary noise of $d_s(n)$. The error signal reflects the control effect and was adopted to update the weight coefficient of $\boldsymbol{w}(n)$.

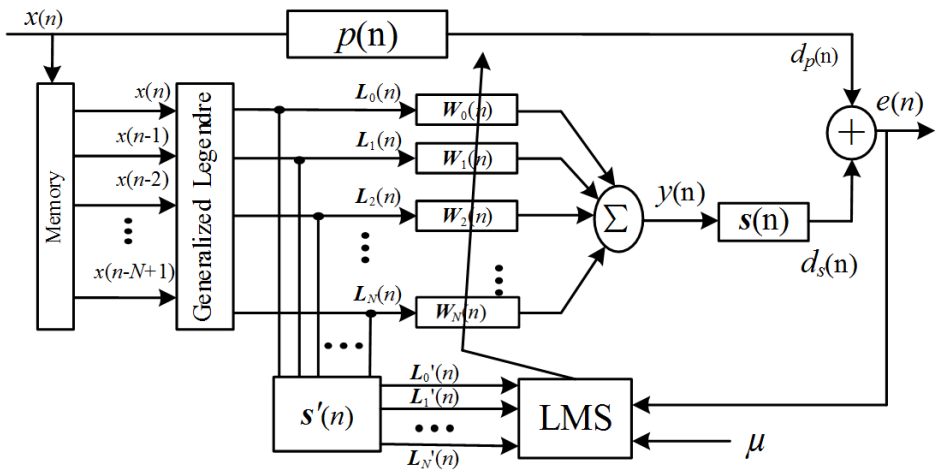

FIGURE 2. Adaptive filtered-x LMS algorithm

From Figure 2, the secondary noise of $d_s(n)$ is symbolized as

$$d_s(n) = \boldsymbol{s}(n) * y(n) \tag{4}$$

where $\boldsymbol{s}(n)$ is the real transfer function for secondary path, and $*$ denotes convolution.

The error signal is expressed as

$$e(n) = d_p(n) - d_s(n) \tag{5}$$

Submitting (3) and (4) into (5), the error signal can be rewritten as

$$e(n) = d_p(n) - \boldsymbol{s}(n) * y(n) = d_p(n) - \boldsymbol{s}(n) * \left[\boldsymbol{w}^T(n)\boldsymbol{l}(n)\right] \tag{6}$$

To obtain the optimal weights, the cost function is defined as

$$\xi = E\left[e^2(n)\right] \tag{7}$$

where $E(.)$ is the expectation. In accordance with the LMS criterion, the weight coefficients can be updated by

$$\boldsymbol{w}(n+1) = \boldsymbol{w}(n) + \frac{\mu}{2}\frac{\partial \xi}{\partial \boldsymbol{w}(n)} \tag{8}$$

where μ is the step size, and $\frac{\partial \xi}{\partial \boldsymbol{w}(n)}$ is the general direction of gradient descent. We use instantaneous gradient as the global gradient [15]

$$\frac{\partial \xi}{\partial \boldsymbol{w}(n)} = -2e(n)\frac{\partial d_s(n)}{\partial \boldsymbol{w}(n)} \tag{9}$$

The update rule can be renovated as

$$\boldsymbol{w}(n+1) \approx \boldsymbol{w}(n) - \mu e(n)\frac{\partial d_s(n)}{\partial \boldsymbol{w}(n)} \tag{10}$$

where $\frac{\partial d_s(n)}{\partial \boldsymbol{w}(n)} = \sum_{m=0}^{L-1} \frac{\partial d_s(n)}{\partial y(n-m)} \cdot \frac{\partial y(n-m)}{\partial \boldsymbol{w}(n)}$, and L represents the secondary length.

The weight vector of $\boldsymbol{w}(n)$ is assumed time-varying slowly, that is

$$y(n-m) = \boldsymbol{w}^T(n-m)\boldsymbol{l}[x(n-m)] \approx \boldsymbol{w}^T(n)\boldsymbol{l}[x(n-m)] \tag{11}$$

We achieve

$$\frac{\partial d_s(n)}{\partial \boldsymbol{w}(n)} = \boldsymbol{l}(n) * \boldsymbol{s}'(n) \tag{12}$$

where $\boldsymbol{s}'(n)$ is the estimation of the secondary path.

The update equation of FXLMS for the CRGL filter can be summarized as

$$\boldsymbol{w}(n+1) = \boldsymbol{w}(n) - \mu e(n)\boldsymbol{l}'(n) \tag{13}$$

3.2. **Filtered-error LMS algorithm.** In the FXLMS algorithm, all diagonal kernels are filtered by the secondary estimation, which leads to heavy computational loads for the NANC system. The FELMS structure can efficiently overcome this problem. In the FELMS algorithm, the error signal was filtered by an error filter; meanwhile, the cross kernels only need to be delayed some time.

As depicted in Figure 3, the updating for the FELMS algorithm can be derived as

$$\boldsymbol{w}(n+1) = \boldsymbol{w}(n) - \mu e'(n)\boldsymbol{l}(n-M) \tag{14}$$

where $e'(n) = e(n) * \boldsymbol{a}(n)$ is the filtered error signal, and $\boldsymbol{a}(n)$ is the inversed secondary path and expressed as

$$\boldsymbol{a}(n) = inverse\left[\boldsymbol{s}'(n)\right] = \left[\boldsymbol{s}'_L(n), \boldsymbol{s}'_{L-1}(n), \ldots, \boldsymbol{s}'_1(n)\right] \tag{15}$$

where L is the secondary length to make the error filter casual.

3.3. **Computational complexity.** For the feedforward nonlinear active noise control system, it is assumed that the primary length is N and the secondary length is L. M diagonal channels are maintained. The multiplication operations which need more time to process compared with addition operation for the adaptive FXLMS and FELMS for second-order CRGL filter include the following parts:

1) Multiplication for generating the cross channel kernels of $\boldsymbol{l}(n)$: $M + 2$;

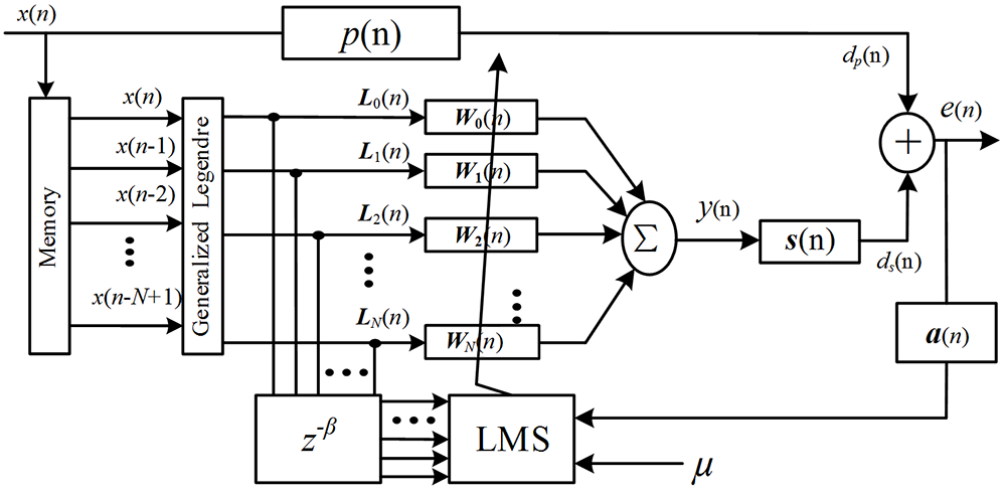

FIGURE 3. Adaptive filtered-error LMS algorithm

2) Multiplication for calculating the control output signal of $y(n)$: $\left(4N-M^2+2MN-M\right)/2$;

3) Multiplication for filtering expanded basis function or error signal, FXLMS: $L(M+2)$ and FELMS: L;

4) Multiplication for updating the weight coefficients: $(6N-M-1)/2+1$.

Table 2 shows the comparison of computational loads required for the second-order Volterra (VFXLMS), FLANN (FSLMS), even mirror Fourier nonlinear (EMFN-FXLMS) and proposed CRGL filters. It is apparent that the Volterra and EMFN filters have almost the same computational loads, while EMFN demands time to generate the sine and cosine base functions. The FELMS algorithm was computationally superior to the FXLMS algorithms. The FSLMS needs the least multiplications, while additional time was needed to generate the sine and cosine base functions.

TABLE 2. Computational loads for different algorithms

Items	CRGL-FXLMS	CRGL-FELMS	VFXLMS/EMFN-FXLMS	FSLMS
Cross term	$M+2$	$M+2$	N	0
Output	$\left(4N-M^2+2MN-M\right)/2$	$\left(4N-M^2+2MN-M\right)/2$	$\left(N^2+3N\right)/2$	$5N$
Filtering	$L(M+2)$	L	$L(N+1)$	$5L$
Updating	$\left(4N-M^2+2MN-M\right)/2+1$	$\left(4N-M^2+2MN-M\right)/2+1$	$\left(N^2+3N\right)/2+1$	$5N+1$
Total	$4N-M^2+2MN+L(M+2)+3$	$4N-M^2+2MN+L+3$	$N^2+4N+L(N+1)+1$	$5N+5L+1$
$N=10$, $L=10$, $M=2$	119	89	251	101
$N=30$, $L=20$, $M=2$	319	239	1641	251

4. **Computer Simulations.** In this section, we designed three different nonlinear experimental conditions and compared the control effect to verify the performance of proposed CRGL filter equipped with adaptive FXLMS and FELMS algorithms. Experiment 4.1 was the control comparison result under the condition of nonlinear logical chaotic noise. Experiment 4.2 showed the control curves of Gaussian noise with the conditions of second-order polynomial primary and secondary paths. Experiment 4.3 was the control performance using the actual primary and secondary paths. For performance comparison, we defined the normalized mean square error (NMSE) as

$$NMSE = 10\lg\left\{E\left\{\frac{1}{K}\sum_{k=1}^{K}\frac{E[e^2(n)]}{\sigma_d^2}\right\}\right\} \tag{16}$$

where σ_d^2 was the energy value of the primary noise at the error sensor, and K was taken as 200. In the following experiments, 2 main diagonal channels were selected for generalized Legendre filter. The register length of filter was chosen to be 10 in Experiments 4.1 and 4.2, 30 in Experiment 4.3.

4.1. **Nonlinear noise source.** The primary noise was nonlinear logistic chaotic noise, which was a commonly used model for validating the filter performance of speech environment, cavity internal noise environment, etc. [3,4]. We generated the logistic chaotic noise using the following formula:

$$x(n+1) = \lambda x(n)[1 - x(n)] \tag{17}$$

where $\lambda = 4$ and $x(1) = 0.9$.

The primary transfer function used in the experiment was defined as

$$P(z) = z^{-5} - 0.3z^{-6} + 0.2z^{-7} \tag{18}$$

The secondary paths of minimum phase and non-minimum phase were given by

$$\begin{aligned} S_m(z) &= \overline{S}(z) = z^{-2} + 0.5z^{-3} \\ S_{n-m}(z) &= \overline{S}(z) = z^{-2} + 1.5z^{-3} - z^{-4} \end{aligned} \tag{19}$$

The step sizes for secondary path with minimum phase were chosen as second-order CRGL-FXLMS and CRGL-FELMS: $\mu_1 = 0.018$, $\mu_2 = 0.006$, second-order VFXLMS: $\mu_1 = 0.028$, $\mu_2 = 0.008$, first-order FSLMS: $\mu_1 = 0.026$, $\mu_2 = 0.006$ and second-order EMFN-FXLMS: $\mu_1 = 0.018$, $\mu_2 = 0.006$, where μ_1 is the step size for linear section of the filter, μ_2 for nonlinear section. For the non-minimum phase secondary path, the steps were second-order CRGL-FXLMS and CRGL-FELMS: $\mu_1 = 0.012$, $\mu_2 = 0.006$; second-order VFXLMS: $\mu_1 = 0.018$, $\mu_2 = 0.006$, first-order FSLMS: $\mu_1 = 0.018$, $\mu_2 = 0.008$ and second-order EMFN-FXLMS: $\mu_1 = 0.018$, $\mu_2 = 0.006$.

Figure 4 showed the control curves of CRGL-FXLMS, CRGL-FELMS, VFXLMS, FSLMS and EMFN-FXLMS algorithms. We can see that the CRGL, Volterra and FLANN filter containing linear components have better control performance than the EMFN filter without linear section. The main reason was that the linear approximate ability of EMFN filter depends on the linear components of the Taylor expansion of sine function. The CRGL filter proposed in this paper achieved better control performance and faster convergence speed under the minimum phase secondary path than the non-minimum phase for the reason of stronger approach ability than prediction.

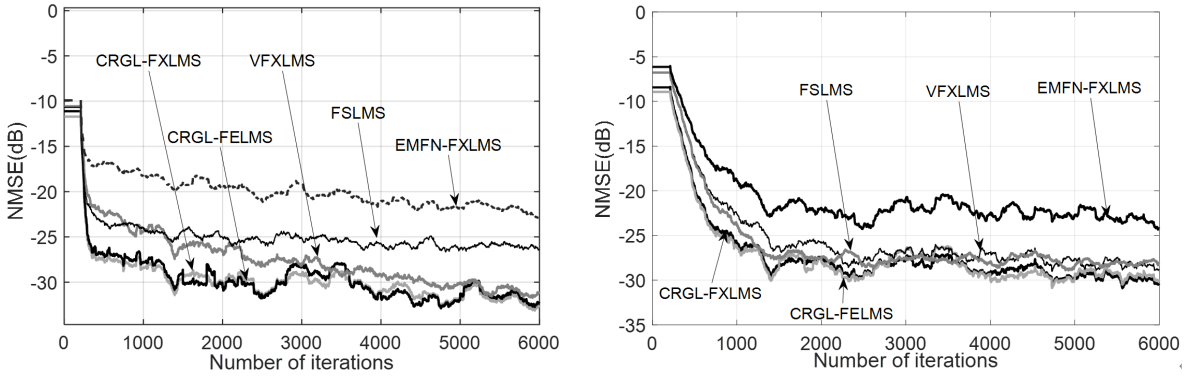

FIGURE 4. Control curves for logistic chaotic noise, secondary path with (a) minimum and (b) non-minimum phase

4.2. **Nonlinear primary and secondary paths.** The second-order polynomial primary and secondary paths were assigned to be nonlinear models in this experiment. The primary path transfer function was defined as

$$d(n) = x(n) + 0.8x(n-1) + 0.3x(n-2) + 0.4x(n-3) - 0.8x(n)x(n-1) + 0.9x(n)x(n-2) + 0.7x(n)x(n-3) \quad (20)$$

The relationship between the secondary signal at the error sensor and the control signal of $y(n)$ was

$$d_s(n) = y(n) + 0.35y(n-1) + 0.09y(n-2) - 0.5y(n)y(n-1) + 0.4y(n)y(n-2) \quad (21)$$

The input noise signal was uniform white noise, and the iteration steps used in the experiment were second-order CRGL-FXLMS and CRGL-FELMS: $\mu_1 = 0.008$, $\mu_2 = 0.004$, second-order VFXLMS: $\mu_1 = 0.008$, $\mu_2 = 0.006$, first-order FSLMS: $\mu_1 = 0.006$, $\mu_2 = 0.004$ and second-order EMFN-FXLMS: $\mu_1 = 0.018$, $\mu_2 = 0.006$.

The comparison of the control performance under nonlinear primary and secondary paths was shown in Figure 5. The CRGL, Volterra and EMFN filters achieved lower mean square error compared with FLANN filter for the cross terms exist. The CRGL filter needs less computational loads than Volterra and EMFN filters.

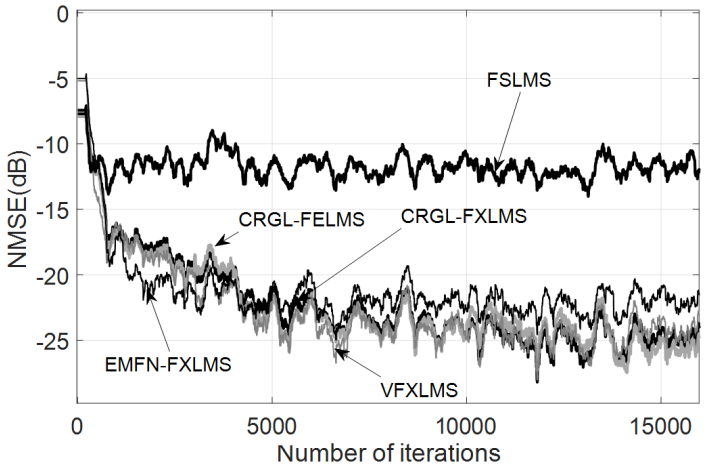

FIGURE 5. Control curves for gauss noise under nonlinear primary and secondary paths

4.3. **Real primary and secondary paths.** A real measured primary and secondary paths [1] were adopted to test the practical performance. The magnitude and phase responses versus frequency of the practical paths were shown in Figure 6. The secondary path was a weak nonlinearity. Three sinewaves at the frequencies of 120 Hz, 360 Hz and 640 Hz were consisted in the reference noise which was normalized to have a unit power. The signal noise ratio (SNR) at the error sensor is set to 40 dB. The steps were second-order CRGL-FXLMS and CRGL-FELMS: $\mu_1 = 0.0006$, $\mu_2 = 0.0006$, second-order VFXLMS: $\mu_1 = 0.0006$, $\mu_2 = 0.0006$, first-order FSLMS: $\mu_1 = 0.0008$, $\mu_2 = 0.0004$ and second-order EMFN-FXLMS: $\mu_1 = 0.0004$, $\mu_2 = 0.0002$.

The NMSE curves were shown in Figure 7. CRGL and Volterra filters have the optimal control performance with the value of about -35 dB for their similar structure. The FLANN filter has poor performance of -23.5 dB for the leak of cross terms. The EMFN filter has a medium performance of -30 dB for the reason that the filter did not contain the linear section in comparison to the CRGL and Volterra filters.

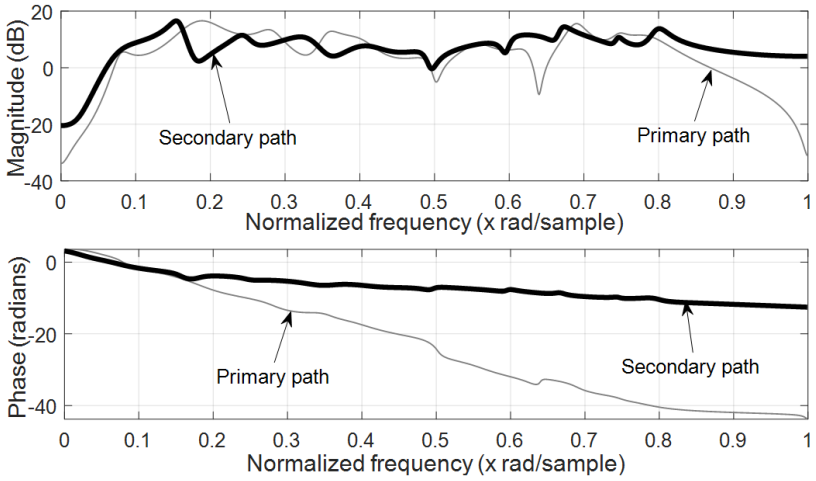

FIGURE 6. Amplitude and phase responses of the actual primary and secondary path

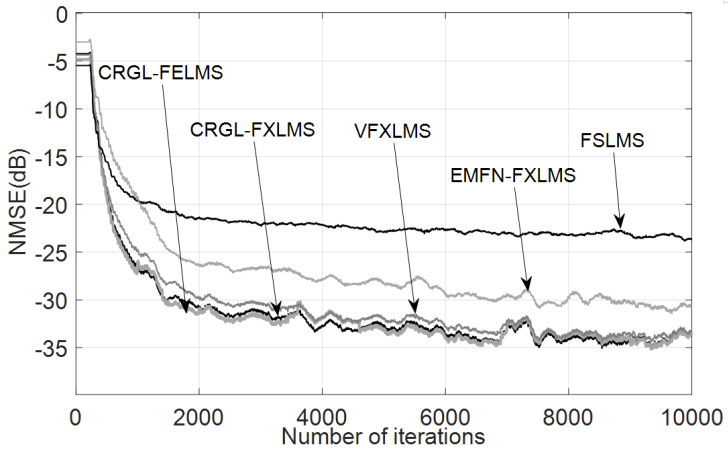

FIGURE 7. Control curves for saturated noise under measured primary and secondary paths

5. **Conclusions.** In this paper, we propose a channel reduced generalized Legendre (CRGL) filter and the corresponding adaptive FXLMS and FELMS algorithms with applications in NANC area. The generalized Legendre filter was developed by adding the cross products to the orthogonal Legendre polynomials based on the Volterra filter. A channel reduced strategy of maintaining dominant channels was adopted to simplify the diagonal channel elements. The computation complexity for CRGL, Volterra, FLANN and EMFN was analyzed and compared. Computer simulation results show the better performance of the proposed filters for nonlinear active noise control system. In the future, the partial update algorithm and normalized step size algorithm could be explored to further reduce the computational loads and achieved faster convergence speed.

Acknowledgment. This work is supported in part by National Natural Science Foundation of China (NSFC) under Project No. 62001183, in part by Jiangsu Agriculture Science and Technology Innovation Fund under Project No. CX(22)3109, and in part by Natural Science Foundation of the Higher Education Institutions of Jiangsu Province under Project Nos. 18JKB14001 and 20KJB510029.

REFERENCES

[1] S. M. Kuo and D. Morgan, *Active Noise Control Systems: Algorithms and DSP Implementations*, John Wiley and Sons, Inc., 1996.

[2] H. Wang, H. Sun, J. Guo, M. Wu and J. Yang, Analysis of the frequency interference in the narrowband active noise control system, *IEEE Trans. Audio, Speech, Lang. Process.*, vol.30, pp.1704-1717, 2022.

[3] L. Tan and J. Jiang, Adaptive Volterra filters for active control of nonlinear noise processes, *IEEE Trans. Signal Process.*, vol.49, no.8, pp.1667-1676, 2001.

[4] D. P. Das and G. Panda, Active mitigation of nonlinear noise processes using a novel filtered-s LMS algorithm, *IEEE Trans. Speech Audio Process.*, vol.12, no.3, pp.313-322, 2004.

[5] Y. Yu, L. Lu, Z. Zheng and X. Yang, Interpolated individual weighting subband Volterra filter for nonlinear active noise control, *IEEE Trans. Circuits Syst. II: Express Brief*, 2022.

[6] X. Guo, J. Jiang, S. Du and L. Tan, Improved adaptive recursive even mirror fourier nonlinear filter for nonlinear active noise control, *Appl. Acoust.*, vol.146, pp.310-319, 2019.

[7] X. Guo, Y. Li, J. Jiang, C. Dong, S. Du and L. Tan, Sparse modeling of nonlinear secondary path for nonlinear active noise control, *IEEE Trans. Instrum. Meas.*, vol.67, no.3, pp.482-496, 2018.

[8] C. Dong, Y. Ding, L. Tan, S. Du and X. Guo, Diagonal-structure adaptive bilinear filters for multichannel active noise control of nonlinear noise processes, *Mech. Syst. Signal Process.*, vol.143, 106703, 2020.

[9] X. Guo, J. Jiang, J. Chen, S. Du and L. Tan, BIBO-stable implementation of adaptive function expansion bilinear filter for nonlinear active noise control, *Appl. Acoust.*, vol.168, 107407, 2020.

[10] D. Le, J. Zhang and D. Li, Hierarchical partial update generalized functional link artificial neural network filter for nonlinear active noise control, *Digit. Signal Process.*, vol.93, pp.160-171, 2019.

[11] A. Carini and G. L. Sicuranza, Legendre nonlinear filters, *Signal Process.*, vol.109, pp.84-94, 2015.

[12] V. Patel, V. Gandhi, S. Heda and N. V. George, Design of adaptive exponential functional link network-based nonlinear filters, *IEEE Trans. Circuits Syst. I: Reg. Papers*, vol.63, no.9, pp.1434-1442, 2016.

[13] B. Chen, R. Guo and K. Zeng, A nonlinear active noise control algorithm using the FEWT and channel-reduced recursive Chebyshev filter, *Mech. Syst. Signal Process.*, vol.166, 108432, 2022.

[14] J. Jiang, V. Vijayarajan and L. Tan, Channel sparsity aware function expansion filters using the RLS algorithm for nonlinear acoustic echo cancellation, *IEEE Access*, vol.8, no.1, pp.118305-118314, 2020.

[15] Z. Luo, D. Shi and W. Gan, A hybrid SFANC-FxNLMS algorithm for active noise control based on deep learning, *IEEE Signal Processing Letters*, vol.29, pp.1102-1106, 2022.